

Autocatalytic Oxidation of Cyclohexane—Modeling Reaction Kinetics

Liquid phase oxidation of hydrocarbons is a major source of organic chemicals. This paper concerns itself with the oxidation of cyclohexane. The process is one in which gas absorption is accompanied by chemical reaction, but little information has been reported. A major factor has been safety considerations, the Flixborough explosion being a constant reminder. In this paper attention is given to the kinetics and to the interaction of kinetics and mass transfer, showing that in this autocatalytic system the dissolved oxygen level rises to saturation and falls as the rate of reaction increases. Initially zero order in oxygen, the reaction becomes first order at low oxygen levels. Oscillations and enhancement due to reaction within the boundary layer are noted. A kinetic model is developed based on simplification of the accepted free radical scheme and it is reasonably successful in accounting for the results reported. Experiments at temperatures up to 170°C and 70 bar using uncatalyzed reaction are reported from three different reactors: a homogenous batch reactor, a flat interface reactor, and a sparged agitated bubbling reactor.

A. K. Suresh, T. Sridhar,
O. E. Potter

Department of Chemical Engineering
Monash University
Clayton, Victoria 3168, Australia

Introduction

The liquid phase oxidation of hydrocarbons is a major source of organic chemicals in the chemical industry. Most of the processes of industrial interest are carried out at pressures of 10–30 bar and temperatures of 353–523 K. In terms of the kinetic mechanisms that operate in liquid phase hydrocarbon oxidations, the liquid phase oxidation of cyclohexane is a typical example of this class of reactions. It is also a reaction of considerable industrial importance. The oxidation of cyclohexane supplies much of the raw materials needed for the production of nylon (both nylon-6 and nylon-6,6)—cyclohexanol, cyclohexanone, and adipic acid. Selective production of cyclohexanol and cyclohexanone requires the use of a low-conversion process with multiple stages. A number of catalysts for the reaction have been reported. Cyclohexanol and cyclohexanone are usually subsequently oxidized with nitric acid to adipic acid.

The kinetic mechanisms that operate in hydrocarbon oxidations in general and cyclohexane oxidation in particular have been quite extensively studied, especially by Russian kineticists (Berezin et al., 1966; Emanuel et al., 1967). However, these mechanistic studies do not lead to rate expressions with con-

stants that can readily be used in the design of industrial reactors. Bearing in mind the way industrial processes operate, these reactions should be studied as gas-liquid reactions in which both mass transfer and reaction kinetics have a role to play. Few studies in the literature have accomplished this. The bulk of available literature (mainly patent literature) discusses the effect on product distribution of operating variables such as temperature, pressure, catalyst, and contacting conditions.

The main products in cyclohexane oxidation are cyclohexyl hydroperoxide, cyclohexanol, cyclohexanone, adipic acid, and water. The formation of water and adipic acid is the result of secondary processes and causes a phase separation at conversions higher than 4–5%. Water has a retarding effect on the reaction and unless the water formed is removed, the oxidation ceases at 25–30% conversion.

Cyclohexyl hydroperoxide is the main primary product in the oxidation. It forms about 1–2% of the oxidate in steel vessels. In the presence of transition metal salts, its decomposition is greatly accelerated and hence much lower concentrations result. The main products of its decomposition are cyclohexanol and cyclohexanone.

Cyclohexanol reaches a maximum concentration of 0.2–0.4 kmol/m³. It is a weak inhibitor of the oxidation process. In the medium of oxidizing cyclohexane, cyclohexanol is converted

A. K. Suresh is presently with Hindustan Lever Research Center, Bombay, India.

almost quantitatively to cyclohexanone. The concentration of cyclohexanone reaches about 0.35–0.6 kmol/m³ during oxidation. It is a highly reactive intermediate and a great variety of oxidation products form from it.

Adipic acid is the main secondary product. The main reactions it enters into in the medium of oxidizing cyclohexane are oxidative decarboxylation (giving valeric and glutaric acids) and esterification with cyclohexanol (giving mono- and dicyclohexyl adipates).

The loss of selectivity that results at higher conversions is due to the high reactivity of the intermediates. Cyclohexanol and cyclohexanone are the intermediates of industrial interest and both are oxidized many times more easily than cyclohexane.

In gas-liquid reactions, a knowledge of intrinsic kinetics is essential for a proper interpretation of experimental data as well as for a rational design of reactors. However, to obtain such information is not easy, particularly in hydrocarbon oxidations, in which high temperatures and pressures are necessary to carry out the reaction. In this work, the intrinsic kinetics of cyclohexane oxidation have been obtained by two methods. In the first, oxygen is dissolved in cyclohexane at room temperature and high pressures in a microautoclave and the latter heated to reaction temperatures. By restricting the conversion to the oxygen dissolved at room temperature, reaction under homogeneous conditions can be ensured. In the second method, kinetics are obtained from gas-liquid reaction studies in the slow reaction regime. The dissolved oxygen concentrations during reaction are measured to make certain that the reaction occurs in the bulk liquid.

Experimental Method

The gas-liquid reactors used have been described by Suresh et al. (1987), where safety aspects also have been discussed. Oxygen absorption rates were measured from the flow rates of oxygen into and out of the reactors. Dissolved oxygen concentration was followed as a function of time. The microautoclaves used in batch studies were of 35×10^{-6} m³ volume and 25×10^{-6} m³ of liquid was charged into them. A fluidized sand bath was used to provide the heating for the microautoclaves. More details of the equipment are available in Suresh (1986). The oxygen conversions based on the initial charge (moles of oxygen consumed per mole of initial liquid) were determined by measuring the volume of the unreacted oxygen under ambient conditions. Cyclohexane conversion and the concentrations of intermediates were determined by gas chromatography as described below.

Chemical Analysis of the Oxidate

Because of the complexity of the reaction scheme, a multitude of products form in cyclohexane oxidation. Various methods are reported in the literature for analyzing the oxidate. Of these, the chromatographic methods seem to be the more promising because of their accuracy and simplicity. Katnik and Johnson (1970) reported a method in which, by silylating the active hydrogen compounds, all the important products could be analyzed in a single analysis. The method cannot detect hydroperoxides, however, and hence is suitable for a catalyzed process in which the hydroperoxide level is known to be negligible.

Although the method of Katnik and Johnson is suitable in principle, it suffers from two disadvantages in the present context. The cyclohexyl hydroperoxide in the samples from the

uncatalyzed oxidation decomposes at the high injection port temperatures used, giving cyclohexanol and cyclohexanone and thereby affecting their quantitation in the sample as well. In addition, the cyclohexanol elutes close to one of the peaks of the silylating agent used and quantitation has to be based on the peak heights rather than on peak areas (Katnik and Johnson, 1970). In the present case, this was found to lead to a poor reproducibility at low concentrations of the cyclohexanol. Good reproducibility was obtained, however, when samples were injected without silylation.

The following modification of the Katnik and Johnson procedure was found to be successful. Any cyclohexyl hydroperoxide is first converted quantitatively to cyclohexanol by addition of a sufficient quantity of triphenylphosphine (TPP). The total cyclohexanol along with cyclohexanone and the unreacted cyclohexane is then estimated by gas chromatography using ethyl acetate as an internal standard. If any analysis for the acids is desired, a portion of the sample is silylated and analyzed again by gas chromatography using benzophenone as an internal standard. The concentration of cyclohexyl hydroperoxide is separately determined by iodometry. This last analysis is quite time consuming, and since the initial results indicated that hydroperoxide concentrations declined rather quickly, it was not extensively used.

The chromatograph was fitted with a thermal conductivity detector. Helium was used as the carrier gas. A 3 m \times 0.003 m column containing 12.5% QF1 on Chromosorb G, followed by a 3 m \times 0.003 m column packed with 3% QF1 on Chromosorb G was used for separating the oxidation products. The following instrumental conditions were used: injection port temperature = 523 K; detector temperature = 523 K; filament current = 170 mA. The oven temperature was held at 298 K for 12 min and then was programmed to rise 4 K/min up to 483 K, where it was held for 8 min. The period of constant initial temperature could be reduced to 2 min if no THF was present in the analysis sample (original sample containing no solids). A Hewlett-Packard integrator recorded and integrated the output from the detector.

Calibrations have been prepared for each of the compounds of interest from the analysis of made up samples. Each sample is analyzed two to three times and the results averaged. With such precautions, an accuracy of better than 0.5% could be achieved for cyclohexane in prepared samples.

Homogeneous Kinetic Studies

The results of chemical analysis of samples from microautoclave runs at 423 and 433 K are shown in Figure 1, but see also Figures 6 and 7. The oxidation of hydrocarbons is expected to be zero order in oxygen at the partial pressures used in these experiments (Berezin et al., 1966; van de Vusse, 1961). The data at 423 K, which show that an increase in the saturation pressure from 20 to 40 bar had no effect on the conversion attained in 105 min, confirm this. The concentrations of cyclohexanol plus cyclohexyl hydroperoxide ($-OL + HP$) and cyclohexanone ($-ONE$) show slightly greater scatter; some error must also be expected in the determination of such small concentrations. This zero-order behavior makes the interpretation of data from these batch experiments simple, since the variation of dissolved oxygen concentration through the experiment can be neglected.

The conversion data fall on a straight line on the semilogarithmic coordinates of Figure 1, giving the relationship between

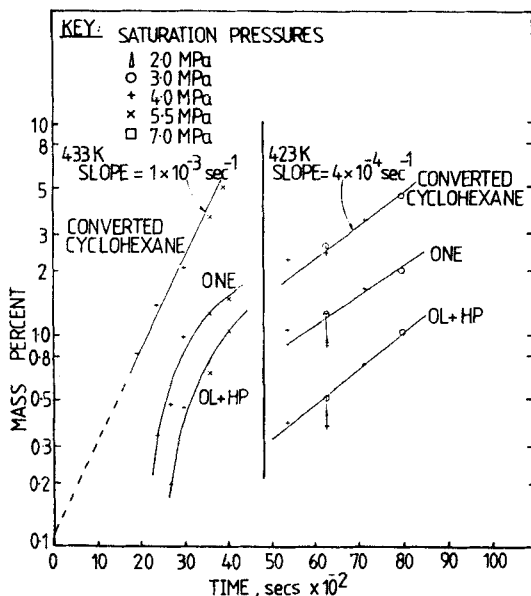


Figure 1. Conversion in homogeneous batch microautoclave at various pressures.

ONE, cyclohexanone; OL+HP, cyclohexanol + cyclohexyl hydroperoxide

cyclohexane conversion X and time t as:

$$\ln (X/X_o) = k_{o1}t \quad (1)$$

Botton et al. (1983) presented such a relationship, which can also be derived from theoretical considerations of the free radical mechanism (Emanuel, 1981). X_o in Eq. 1 is a hypothetical conversion obtained by the extrapolation of the straight line to zero time. An expression can be written for the overall cyclohexane conversion kinetics from the observed zero-order dependence on oxygen and Eq. 1, as:

$$\frac{dX}{dt} = k_{o1}X \quad (2)$$

which shows that the rate of formation of products is first order in the concentration of the products and zero order in oxygen. Equation 2 represents an autocatalytic process in which all the products can be lumped together in their autocatalytic effect. In the sequence of reactions postulated for the oxidation of cyclohexane (Berezin et al., 1966), most products of the early stages of reaction are capable of accelerating the process. It is therefore not surprising that such a result should obtain at low conversions, when the secondary stages of the reaction, which lead to unreactive final products, are of minor importance. As such products build up, Eq. 2 may be expected to overestimate the rates. Equation 2 also does not apply in the very low conversion region (i.e., during the induction period), since at $X = 0$ it predicts the physically unrealistic rate of zero. Despite these limitations, Eq. 2 provides a simple expression of the overall kinetics in this complex free radical process, and will be shown to be useful in the conversion range of industrial interest.

The product analyses show, Figure 1, that the cyclohexanone is in higher concentration than the sum of cyclohexanol and cyclohexyl hydroperoxide at all conversions. This result is in

good agreement with several studies in the literature (Berezin et al., 1966; Takamitsu and Hamamoto, 1972). If a straight-line representation is used for these data also, the resulting lines have slopes very similar to that of total conversion.

In Figure 2, the oxygen conversion is plotted as a function of batch time, in semilogarithmic coordinates. The independence of oxygen conversion rates on the oxygen concentration is seen in this figure also. The relationship is linear in the conversion range studied. If the data are fitted by straight lines, the slopes of these lines are very similar to the corresponding lines in Figure 1. Over the conversion range covered by the data, the moles of cyclohexane converted agree fairly satisfactorily with the moles of oxygen taken up, indicating a stoichiometry of 1 for the overall reaction between oxygen and cyclohexane in this conversion range. Although the low conversion data at 433 K seem to indicate that less than one mole of oxygen is consumed per mole of cyclohexane converted (and this is not impossible, since the primary intermediates, cyclohexanol and cyclohexanone, each contain only half a mole of oxygen per mole), experimental errors in both conversion as well as oxygen uptake measurements in this region make it difficult to conclude that this is the case. Berezin et al. state that an oxidation conversion of 4.3% requires about 1 mol oxygen/mol cyclohexane; such is seen to be approximately the case.

Dosing Studies

This section describes studies on the oxidation kinetics in the presence of the main reaction intermediates, cyclohexanol and cyclohexanone.

Figure 3 shows the results of batch studies at 423 K with 4.04 mol % cyclohexanol in the feed. The cyclohexane conversion is shown at different batch times. Since chemical analysis gives the total amount of products in the sample including the amount added initially, the conversions plotted are total conversions.

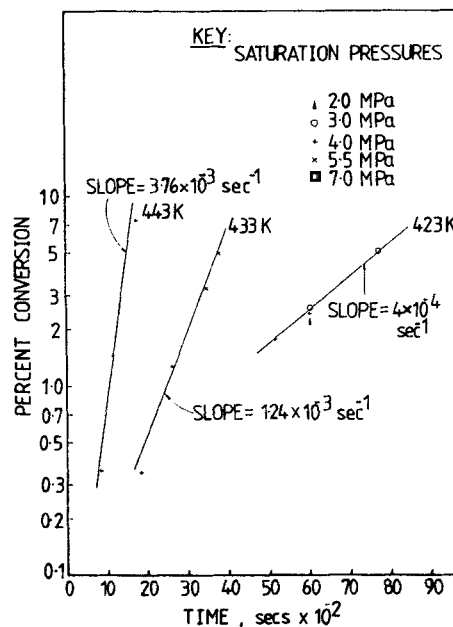


Figure 2. Oxygen conversion kinetics at various temperatures in microautoclave under homogeneous conditions.

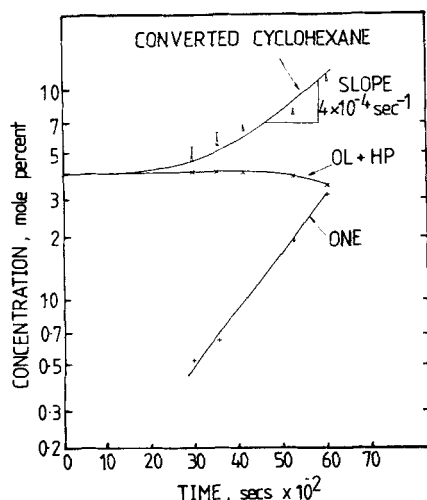


Figure 3. Dosing studies: effect of cyclohexanol in feed on cyclohexane conversion and product formation.

423 K, homogeneous batch reaction

After an initial induction period, the data show a tendency toward linearity, with the slope being equal to that obtained with pure cyclohexane. In other words, the cyclohexanol (which is one of the reaction products) added initially has the same effect on the oxidation rate as an equal concentration of products formed from the oxidation of pure cyclohexane, as anticipated by Eq. 2.

The oxygen conversion data from the same series of runs are shown in Figure 4 on log linear coordinates. It is seen that if the oxygen conversions as experimentally measured are fitted by a straight line, the slope is much higher than that obtained with pure cyclohexane, showing the catalytic effect of cyclohexanol. However, when the product initially present is added as an equivalent conversion at zero time and the total conversions plotted, the points fall on a straight line, the slope of which is

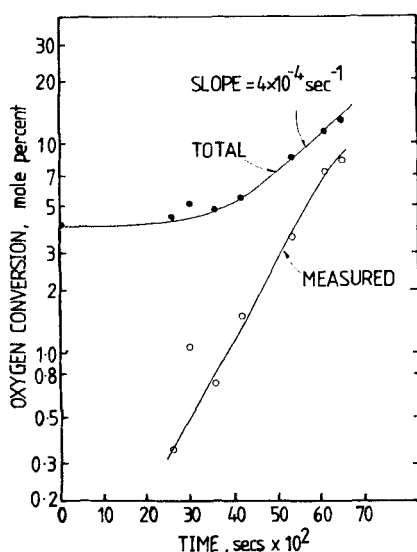


Figure 4. Dosing studies: effect of 4.04 mol % cyclohexanol in feed on oxygen conversion rates.

423 K, homogeneous batch reaction

identical to the rate constant obtained with pure cyclohexane. This shows once again that cyclohexanol is as effective as an equal concentration of total oxidation products in enhancing the rate.

It is seen that even though the added cyclohexanol increases the rates in pure cyclohexane (to what would otherwise be obtained at an equal oxidation conversion), it is hardly effective in reducing the induction period. Since the induction period is the time required for a sufficient concentration of free radicals to form, this would indicate that cyclohexanol, even though more reactive than cyclohexane, is almost as sluggish in forming free radicals.

The moles of cyclohexanol and cyclohexanone at different reaction times have also been plotted in Figure 3. Cyclohexanol, having been added at the start in amounts close to the maximum concentration it attains in normal oxidation, does not accumulate significantly, its concentration remaining almost constant initially and showing a decrease at higher conversions. Cyclohexanone, which forms from cyclohexanol in the medium of oxidizing cyclohexane, forms rapidly, its rate of formation increasing with time.

Studies at 423 K with cyclohexanone in the feed are summarized in Figure 5. The oxygen conversion data have been obtained with either 4.12 or 7.91 mol % cyclohexanone in the feed. The induction period is seen to have considerably shortened, showing that, unlike cyclohexanol, cyclohexanone can form free radicals with considerable facility. Both oxygen and cyclohexane conversions, when plotted as total conversions including the cyclohexanone added initially, are once again fitted well by the rate constant for pure cyclohexane in the region after the induction period up to conversions of 13%. The results show that cyclohexanone (like cyclohexanol) is as effective in increasing the oxidation rates as an equal concentration of total reaction products.

Kinetics from Gas-Liquid Reaction Studies

Beyond a certain conversion, the reaction rate is sufficiently high for mass transfer limitations to be taken into account. The occurrence of reaction in the bulk liquid can be recognized by the presence of nonnegligible amounts of dissolved oxygen in the bulk liquid. Under these conditions (the slow reaction regime)

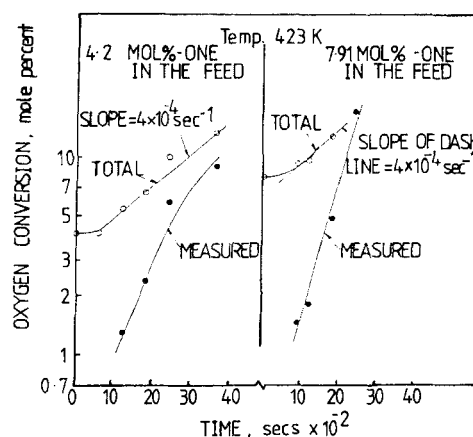


Figure 5. Dosing studies: effect of cyclohexanone in feed on oxidation kinetics.

423 K, homogeneous batch reaction

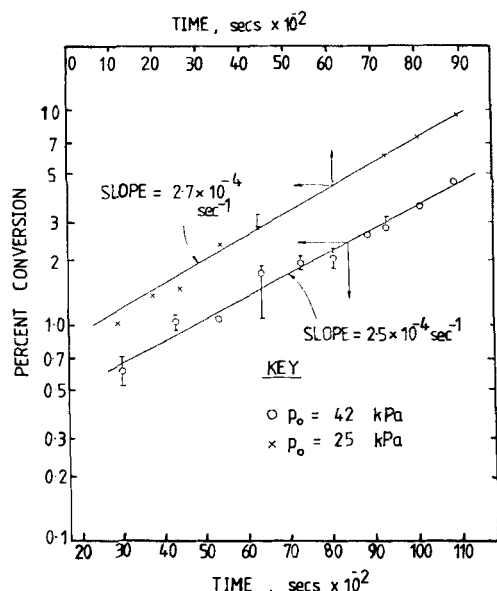


Figure 6. Cyclohexane conversion kinetics at 413 K, heterogeneous stirred-tank reactor.

mass transfer and chemical reaction occur in series (Astarita, 1967) and intrinsic kinetics can be obtained.

Cyclohexane conversions in the slow reaction regime are plotted in Figures 6 and 7. The entire data set covers a temperature range of 413–433 K and different inlet levels of oxygen and contacting conditions. The linear dependency of the logarithm of conversion on time is seen in all cases.

The zero-order dependence of cyclohexane conversion kinetics on oxygen is seen by the fact that the straight lines at a given temperature have the same slope. If induction periods could be reproduced, the corresponding data points would fall on the same straight line, as shown by the results from two experiments at 423 K, conducted with oxygen partial pressures of 0.57 and 0.70 bar at the reactor inlet, Figure 7. Viewing these results in conjunction with the results of the homogeneous kinetic studies,

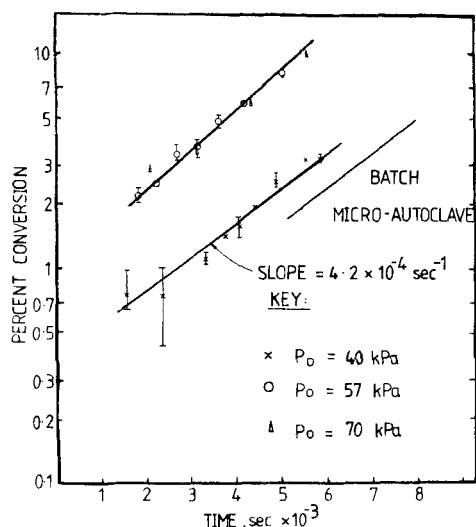


Figure 7. Cyclohexane conversion kinetics at 423 K, heterogeneous stirred-tank reactor.

which also showed zero-order kinetics, but at oxygen partial pressures about an order of magnitude higher than those used in the stirred-tank reactor (STR) studies, it can be concluded that the zero-order behavior of the kinetics with respect to oxygen extends down to quite low concentrations.

Since the present data and those presented earlier have both been obtained under kinetically controlled conditions, and since the concentration of oxygen has been shown not to influence the kinetics, the rate constants in Eq. 2 recovered from either set of data must be the same.

The present data show the cyclohexane conversion kinetics to follow Eq. 2 in the conversion range of 1–10%. A model will be developed that will explain these kinetic features.

Using the data obtained over the temperature range of 413–433 K, the rate constant k_{01} is plotted in Figure 8 as a function of reciprocal temperature, and the data are seen to show an Arrhenius-type dependency on temperature. The equation for the rate constant from Figure 8 is

$$k_{01} = 8.6 \times 10^{10} \exp \left(\frac{-115.2 \times 10^6}{RT} \right) \quad (3)$$

showing an activation energy of 115.2×10^6 J/kmol, which is typical for a kinetically controlled process.

Reaction rate of oxygen as a function of conversion

The reaction rate of oxygen can be calculated from the measured absorption rate as

$$r_o = \frac{R_A}{H_L} - \frac{dc_L}{dt} \quad (4)$$

The reaction rate of oxygen so calculated (the second term on the righthand side is usually negligible in comparison to the others so that a pseudosteady state assumption can be made) has been plotted as a function of conversion in Figure 9 for different temperatures, contacting conditions (hence volumetric mass transfer coefficients), and inlet oxygen partial pressures. The mass transfer coefficients shown in the figures are the values obtained from the data in the slow reaction regime (Suresh et al., 1987). The reaction rates are seen to correlate very well with conversion at a given temperature in the initial part of the experiments. The approximate point at which zero dissolved oxygen concentration was achieved in these experiments has been indicated on the curves, and it is seen that shortly before this time

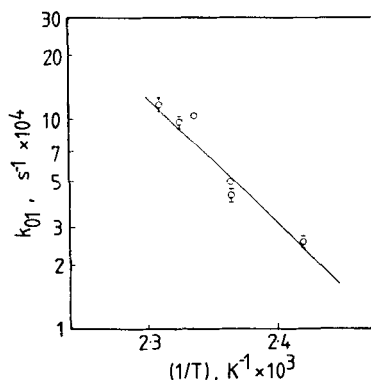


Figure 8. Activation energy plot for k_{01} .

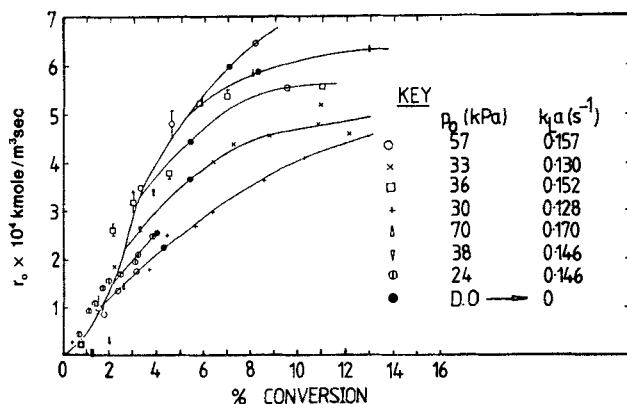


Figure 9. Reaction rate of oxygen as a function of cyclohexane conversion, 423 K.

the reaction rates begin to depend on the $k_L a$ and oxygen partial pressure in addition to the conversion. Since hydrocarbon oxidations are expected to become first order in oxygen in the limit of small oxygen concentrations, such a result is not unexpected. The oxygen reaction rates beyond the zero dissolved oxygen concentration either level off or (in cases where a rate enhancement was observed) show a slower rate of increase than before. As the dissolved oxygen concentrations approach zero, the absorption rates increase much more slowly. The diffusion-limited rate is approached asymptotically since the reaction is first order in oxygen in the limit of low oxygen concentrations.

The independence of reaction rates on oxygen partial pressure in the initial part of the curves in Figure 9 confirms that the kinetics are zero order in oxygen in this region, as are the cyclohexane conversion kinetics. However, while the reaction rate of cyclohexane was found to be first order in total conversion, Eq. 2, Figure 9 suggests that the dependency of r_o on conversion is more likely to follow a parabolic law.

Kinetic Model for Oxidation of Cyclohexane

In this section, the free radical chain mechanism of cyclohexane oxidation is interpreted in the light of experimental findings and a simple kinetic model is derived.

In the free radical mechanism of hydrocarbon oxidation the oxidation products are themselves capable of forming and reacting with free radicals. As a first approximation, we can assume that all the products formed during the oxidation of cyclohexane can participate in the radical initiation and propagation of reactions. Such an assumption may not be far in error at the low conversions being considered, and the observed correlation of the kinetic rates with total conversion supports this.

Derivation of the simplified kinetic equation is presented in appendix A. Equations for cyclohexane and oxygen conversion rates are given by Eqs. A13 and A14.

Limiting cases

Zero-order Kinetics. At high values of c_L , $k_3 c_L$ is the dominant term in the denominator in Eqs. A13 and A14, hence we have for the rates of cyclohexane and oxygen conversion:

$$r_{cz} = \frac{dc_P}{dt} = k_{01} c_P \quad (5)$$

$$r_{oz} = k_{01} c_P + k_{02} c_P^2 \quad (6)$$

Equations 5 and 6 show that the conversion rates are zero order in oxygen in the limit of high oxygen concentrations. The form of Eq. 5 has been confirmed earlier for cyclohexane conversion kinetics and hence the rate constant k_{01} can be identified with the constant introduced in Eq. 1. The plots of oxygen reaction rate as a function of conversion indicate a rate expression of the above form in the region of zero-order kinetics.

First-order Kinetics. In the limit of very low oxygen concentrations, Eqs. A13 and A14 simplify respectively to:

$$r_{c1} = \frac{k_{01} k_3}{(k_{01} + k_{02} c_P)} c_P c_L \quad (7)$$

and

$$r_{o1} = k_3 c_P c_L \quad (8)$$

Equations 7 and 8 show that the kinetics become first order in oxygen at low concentrations of dissolved oxygen. A critical concentration of oxygen below which the first-order asymptotic solutions apply can be defined by equating the zero- and first-order rates and solving the resulting equation for the concentration of oxygen:

$$c_{Lc} = \frac{k_{01} + k_{02} c_P}{k_3} \quad (9)$$

Although the transition from zero to first order does not occur abruptly at c_{Lc} , Eq. 9 does indicate that the first-order transition occurs at higher dissolved oxygen concentrations at higher conversions. In other words, realization of zero-order kinetics at higher conversions requires operating at higher values of the dissolved oxygen concentration.

Rate of accumulation of intermediates

Consider the overall reaction as two consecutive reactions in series. According to this scheme, cyclohexane goes to the intermediates (cyclohexyl hydroperoxide, cyclohexanol, and cyclohexanone) in the first step, and the intermediates react further in the second step to form secondary products. It is further assumed that the intermediates formed are consumed by reactions given by Eqs. A3 and A4 involving peroxy radicals. Since the intermediates form from cyclohexane, the rate of their formation is equal to the rate of conversion of cyclohexane. Since PH in Eq. A4 stands for any product, intermediate or secondary, and since all products have been assumed to react with the peroxy radicals at the same rate, the rate of consumption of the intermediates can be obtained by multiplying the total rate of the reaction, Eq. A4, by the factor (c_I/c_P) , c_I being the concentration of the intermediates. These arguments lead to

$$r_i = \frac{dc_I}{dt} = k_3 c_P c_L \frac{(k_{01} - k_{02} c_I)}{(k_{01} + k_{02} c_P + k_3 c_L)} \quad (10)$$

for a system that is closed with respect to these intermediates. Equation 10 can also be derived by a consideration of the propagation reactions by assuming that, in reactions given by Eq. A3 or A4, the reactions that involve the cyclohexylperoxy radical

lead to the intermediates, while those that involve a peroxy radical from any of the products lead to a secondary product. This assumption is not an unreasonable one, since a molecule of cyclohexyl hydroperoxide (HP) results when a cyclohexylperoxy radical abstracts an atom of hydrogen from a hydrocarbon. HP, besides being an intermediate in the scheme considered, is also a precursor of the other two intermediates, cyclohexanol and cyclohexanone. On the other hand, various secondary products form from the hydroperoxide of cyclohexanone (for example), which is the result of hydrogen abstraction by a peroxy radical that forms from cyclohexanone. However, Eq. 10 does not predict a decrease in the concentration of intermediate, which is expected at high conversions (as the intermediates accumulate, the predicted rate of accumulation of the intermediates goes to zero and remains at zero at higher conversions). Hence, this equation may be valid only at low conversions; but this is a limitation of all the equations derived in this section, the entire kinetic model having been suggested by the experimental data at low conversions. A study of the experimental data presented in the various figures in this paper will show that a significant downturn in the concentration of the intermediates was not observed in the range of conversions studied, while an extended plateau was often observed, as predicted by Eq. 10.

Application of Model to Batch Oxidation in a STR: Slow Reaction Regime

The coupled mass balance equations for the gas and liquid phases, for physical mass transfer are easily extended to the case of a slow reaction taking place in the liquid bulk. There is no enhancement of the mass transfer under these circumstances. Mathematical details are given in appendix B.

Estimation of Kinetic Parameters

The kinetic model has three kinetic constants, k_{01} , k_{02} , and k_3 , which have to be determined by matching the experimental concentration and rate of absorption profiles in the slow reaction regime with the solutions to Eqs. B7–B10. We have seen that an estimate for k_{01} can be obtained by fitting the concentration-time data to Eq. B12. An accurate estimate of k_3 is hard to obtain, first because the dissolved oxygen concentration in which the reaction is first order in oxygen is very small, and second because of the oscillations for dissolved oxygen. An estimate for k_{02} was obtained by considering the initial part of the rate (or dissolved oxygen) vs. time data (data in the region corresponding to the common envelope in Figure 9) to be represented by the solutions for zero-order kinetics, and trying out different values of k_{02} to obtain a good fit. With these estimates, the rate and dissolved oxygen data (which are related through the volumetric mass transfer coefficient) in the entire slow reaction regime were fitted by trying different values of k_3 and solving differential Eqs. B7–B10. With these parameters, the concentration of the intermediates was predicted as a function of time using Eq. B10 and compared with the experimental data. The differential equations were solved using the subroutine DGEAR (IMSL, Inc.). The numerical integration could be checked in the region of high dissolved oxygen concentrations using the analytical solutions, Eqs. B12 and B13.

Parametric sensitivity

The effects on the predictions of the model of varying k_{02} or k_3 are illustrated in Figures 10 and 11. The value of the constant

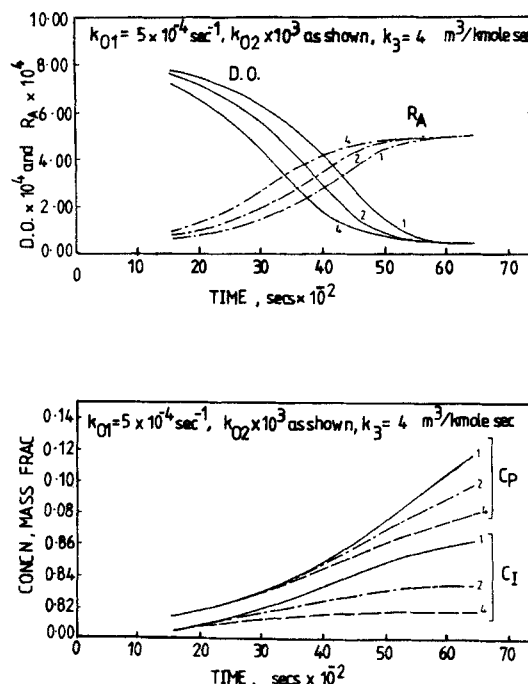


Figure 10. Sensitivity of model predictions to k_{02} .
Top. Variation of dissolved oxygen and absorption rate
Bottom. Variation of products' concentration and intermediates' concentration: k_{02} same units as k_1 .

k_{01} as well as the other parameters such as mass transfer coefficient employed in these calculations were typical values obtained experimentally at 423 K. The values of k_{02} and k_3 have also been varied around the values that fit the experimental data at 423 K. The rate constants have the following units: k_{01} is in

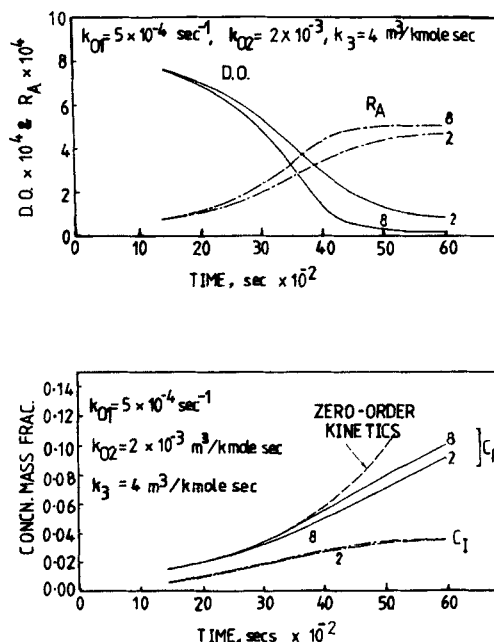


Figure 11. Sensitivity of model predictions to k_3 .
Top. Variation of dissolved oxygen and absorption rate
Bottom. Variation of products' concentration and intermediates' concentration

s^{-1} and k_{02} and k_3 , in $m^3/kmol \cdot s$. In interpreting these curves it should be remembered that the absorption rate and the dissolved oxygen level at any time are representative of the instantaneous kinetic rates at that time, while the total product and intermediate compositions represent an accumulated effect of reaction up to that time.

The effect of a change in k_{02} is shown in Figures 10a and 10b. From Figure 10a it is seen that the effect of a change in k_{02} is minimal at small and large times. At small times, this is due to the fact that the term containing k_{02} in the oxygen conversion kinetics is second order in the concentration of products and is therefore unimportant at small conversions. This is also the reason why the stoichiometry is observed to be unity at small conversions. At large times, the kinetics are first order in oxygen (because c_L is small), the kinetic rates in the bulk of the liquid go asymptotically down to zero, and the process becomes diffusion-limited. The final constant absorption rate is the rate of physical absorption at maximum driving force corresponding to the oxygen level at the exit.

The effect of a change in k_{02} on the conversion and the concentration of the intermediates is seen in Figure 10b. Higher values of k_{02} , since they promote oxygen consumption by the products in preference to that by cyclohexane, result in lower conversions, especially in the constant absorption rate period. For the same reason, the intermediates' concentration is less at equal conversions at higher values of k_{02} (the rate of consumption of the intermediate is increased).

The effect of k_3 is shown in Figures 11a and 11b. As expected, the effect is maximum in regions where the first-order component of the kinetics becomes important. Compared to the effect it has on the R_A - t and c_L - t curves, a change in k_3 has comparatively little effect on the shapes of the c_P - t and c_I - t curves. The conversion-time curve for $k_3 = \infty$ is also shown, which represents the case of zero-order kinetics holding throughout. Comparing this curve with the one for $k_3 = 8,000$ we see that, provided the value of k_3 is not too small, the zero-order assumption is good up to approximately the time at which dissolved oxygen is nearly zero. This justifies the method employed for the estimation of k_{01} , which assumes Eq. B11 to hold in this region. The small sensitivity of the X - t data to the value of k_3 explains why, even though a slowing down of the rate of increase of R_A is readily recognized in the plots of r_o vs. X , Figure 9, the plots of $\ln X$ vs. time, Figures 6 and 7, remain linear nearly up to the time the dissolved oxygen goes to zero. The small deviation from linearity would not be distinguishable from experimental scatter.

Studies on the sensitivities of the model predictions to the values of k_{02} and k_3 at other values of k_{01} (that correspond to the other temperatures covered in this work) revealed similar trends.

Comparison of model predictions with experimental results

In Figures 12, 13, and 14 the predicted profiles of dissolved oxygen, absorption rate, and the concentrations of total products and intermediates are compared with the experimental curves from a few typical experiments over the temperature range 413–433 K conducted under various conditions of gas-liquid contacting and inlet oxygen partial pressures. At each temperature, a single set of values for the rate constants has been used to simulate all the runs. Where values of k_{01} estimated from the semi-logarithmic plot of conversion-time data vary over a range, the

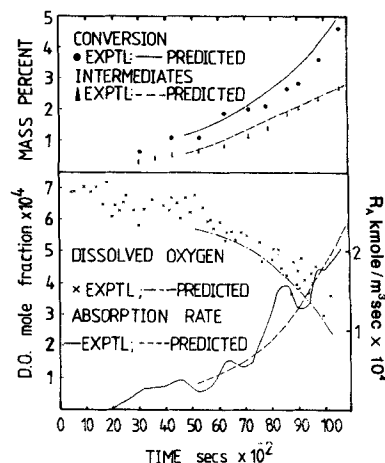


Figure 12. Model predictions and experimental results at 413 K.

$$\begin{aligned} p_o &= 0.42 \text{ bar,} & k_{La} &= 0.12 \text{ s}^{-1} \\ k_{01} &= 2.6 \times 10^{-4} \text{ s}^{-1} & k_{02} &= 1.2 \times 10^{-3} \text{ m}^3/\text{kmol} \cdot \text{s} \\ k_3 &= 4 \text{ m}^3/\text{kmol} \cdot \text{s} \end{aligned}$$

value that best fitted all the sets of data available has been used in the model calculations. The data being compared with the model predictions are from the slow reaction regime in the experiments, as evidenced by the presence of dissolved oxygen in the liquid. The curve for intermediates in these figures represents the total of cyclohexanol, cyclohexyl hydroperoxide, and cyclohexanone. In generating the theoretical curves, a nonzero initial time has to be chosen, since the kinetic equations are valid

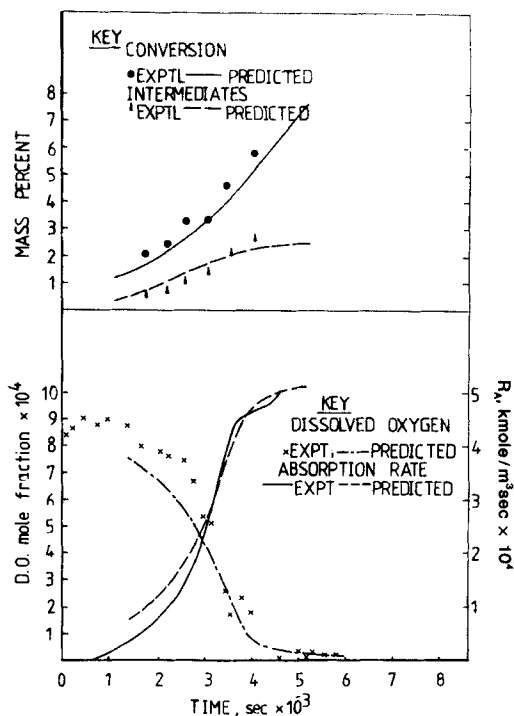


Figure 13. Model predictions and experimental results at 423 K.

$$\begin{aligned} p_o &= 0.57 \text{ bar,} & k_{La} &= 0.151 \text{ s}^{-1} \\ k_{01} &= 5 \times 10^{-4} \text{ s}^{-1} & k_{02} &= 3 \times 10^{-3} \text{ m}^3/\text{kmol} \cdot \text{s} \\ k_3 &= 10 \text{ m}^3/\text{kmol} \cdot \text{s} \end{aligned}$$

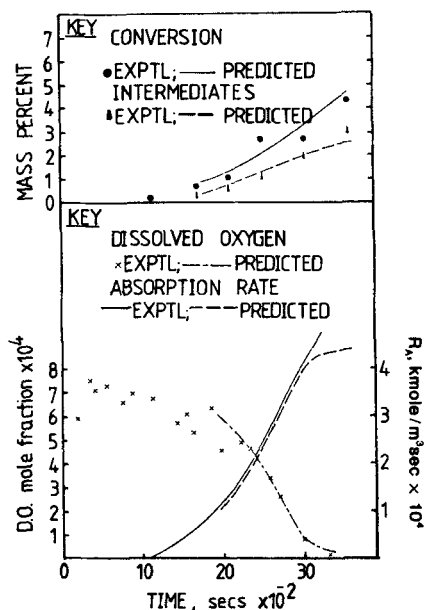


Figure 14. Model predictions and experimental results at 428 K.

$$\begin{aligned} p_o &= 0.46 \text{ bar} & k_L a &= 0.14 \text{ s}^{-1} \\ k_{o1} &= 10.34 \times 10^{-4} \text{ s}^{-1} & k_{o2} &= 5 \times 10^{-3} \text{ m}^3/\text{kmol} \cdot \text{s} \\ k_3 &= 15 \text{ m}^3/\text{kmol} \cdot \text{s} \end{aligned}$$

only beyond a minimum conversion. This initial conversion has been taken for the purpose of these simulations as around 1%, since the reliability of the conversion and rate data at smaller conversions is considered to be poor.

The predictions of the model are seen to be quite good in general. The model is able to account satisfactorily for the effect of the diverse contacting conditions and inlet partial pressures of oxygen. The discrepancies in the prediction of rate and conversion, in some cases, increase toward the end of the slow reaction regime. These cases were mostly those in which a mass transfer enhancement was observed at longer times.

In many cases, the theoretical curve showing the variation of intermediates' concentration with time shows a tendency to level off at lower concentrations than the experimental. It is possible that the model overestimates the rate at which intermediates are consumed, since all the intermediates have been supposed to yield secondary products by reaction with the peroxy radicals. In reality, some intermediates react to give other intermediates; thus, cyclohexyl hydroperoxide yields cyclohexanol and cyclohexanone, and cyclohexanol yields cyclohexanone. Incorporation of these details into the model was not considered in this work since the data required for comparison have not been obtained (only the total concentration of cyclohexanol and cyclohexyl hydroperoxide has been determined in this work). Over most of the concentration range achieved in the slow reaction regime, the agreement between theoretical and experimental curves is seen to be fairly satisfactory.

Effect of Temperature on Kinetic Constants

With the values of the kinetic parameters having been estimated over a range of temperatures, the effect of temperature on these parameters can now be investigated. k_{o1} was shown to obey the Arrhenius equation with an activation energy of $115.2 \times 10^6 \text{ J/kmol}$. The rate constant k_{o2} has been plotted

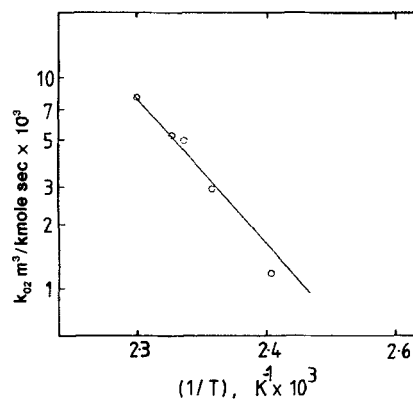


Figure 15. Activation energy plot for k_{o2} .

against reciprocal temperature in Figure 15. The linear fit is satisfactory. The equation given by the straight line in the figure is:

$$k_{o2} = 3.67 \times 10^{16} \exp(-130.4 \times 10^6/RT) \quad (11)$$

and for k_3 it was found that

$$k_3 = 9.63 \times 10^{17} \exp\left(\frac{-113.4 \times 10^6}{RT}\right) \quad (12)$$

The activation energies for the constants k_{o2} and k_3 are seen from these equations to be respectively 130.4 and $113.4 \times 10^6 \text{ J/kmol}$. It must be mentioned that the values (hence also the activation energy) of the kinetic constant k_3 are substantially less accurate than those of the other two constants.

Conclusions

The reaction is confirmed as autocatalytic with the rate of conversion of cyclohexane proportional to the concentration of products. As a consequence, in the stirred-tank reactor the dissolved oxygen level decreases with time as the reaction rate increases. In the flat interface reactor this decrease is very rapid due to a low ratio of mass transfer surface to volume. At higher levels of oxygen concentration the reaction is zero order in oxygen level. At lower oxygen concentrations the data reveal a tendency to undergo oscillations. Such oscillations will be discussed in a later paper. A detailed study of selectivity has not been made, but in the homogeneous reactor the cyclohexanone is found to be in higher concentration than the sum of cyclohexanol and cyclohexyl hydroperoxide at all conversions.

The kinetic model is able to account for the transition in kinetics from zero-order dependence on oxygen at high concentrations to first-order dependence at low concentrations and is able to predict with reasonable accuracy the development of the concentration of total products as well as of total intermediates. The model considers all the intermediates as one lump and hence cannot explain the differences in the cyclohexanol to cyclohexanone ratio found between the data from the diffusional regime and the data from the kinetic regime. Activation energies have been found for the three kinetic constants and the difference in activation energy between k_{o1} and k_{o2} could explain a slight decrease in selectivity as temperature is increased.

Notation

a = interfacial area per unit volume of dispersion, m^2/m^3
 A = dimensionless group, $k_1 a \tau_G$
 B = dimensionless group, $\beta V_L / N_G$
 c = concentration, kmol/m^3
 c_L = concentration of dissolved gas (or oxygen) in bulk liquid, kmol/m^3
 c_{Lc} = critical value of oxygen concentration below which oxidation is first order in oxygen, kmol/m^3
 c_{Lo} = oxygen concentration in liquid in initial steady state in step-change experiments
 c_P = product concentration in liquid, kmol/m^3
 c_R = concentration of cyclohexane in bulk liquid, kmol/m^3
 c_i^* = value of c^* at partial pressure at contractor outlet, if all oxygen entering the reactor were to leave without any being absorbed, kmol/m^3
 c_o^* = value of c^* at prevailing partial pressure at contractor outlet, kmol/m^3
 C_R = concentration of cyclohexane, kmol/m^3
 C = dimensionless rate constant, k_{01}/k_{La}
 D = dimensionless rate constant, $k_{02} c_i^* / k_{La}$
 f_i = functional relationship between rate of initiation and concentration of free radicals, f_i same for termination
 F = dimensionless rate constant, $k_3 c_i^* / k_{La}$
 G_1 = total molar flow rate of gases at inlet of contractor, kmol/s
 G_2 = total molar flow rate of gases at outlet of contractor, kmol/s
 H_L = fractional liquid holdup
 k = first-order rate constant, s^{-1}
 k_{01} = rate constant in expression for cyclohexane conversion rate, s^{-1}
 k_{02} = overall rate constant, $\text{m}^3/\text{kmol} \cdot \text{s}$
 k_3 = overall rate constant $\text{m}^3/\text{kmol} \cdot \text{s}$
 k_p = elementary reaction rate constant for propagation reaction of a primary free radical with oxygen, $\text{m}^3/\text{kmol} \cdot \text{sec}$
 k_{p1} = elementary reaction rate constant for propagation reaction of a peroxy radical with cyclohexane, $\text{m}^3/\text{kmol} \cdot \text{sec}$
 k_{p2} = elementary reaction rate constant for propagation reaction of a peroxy radical with a product, $\text{m}^3/\text{kmol} \cdot \text{sec}$
 k_{La} = volumetric mass transfer coefficient, per unit dispersion volume, s^{-1}
 K = constant of proportionality between total radical concentration and total product concentration
 N_G = number of moles of gas in contactor (in a bubbling contactor, number of moles of gas dispersed as bubbles)
 O_2 = oxygen molecule
 PH = reaction product, hydrocarbon
 r_c = rate of reaction of cyclohexane, $\text{kmol}/\text{m}^3 \cdot \text{s}$, subscript z for zero-order kinetics
 r_i = rate of accumulation of intermediates, $\text{kmol}/\text{m}^3 \cdot \text{s}$
 r_o = rate of reaction of oxygen, $\text{kmol}/\text{m}^3 \cdot \text{s}$, subscript z for zero-order kinetics
 r_{ini} = rate of initiation of free radicals, $\text{kmol}/\text{m}^3 \cdot \text{s}$
 r_{ter} = rate of termination of free radicals, $\text{kmol}/\text{m}^3 \cdot \text{s}$
 R = universal gas constant, $\text{J}/\text{kmol} \cdot \text{K}$
 R_A = oxygen absorption rate per unit dispersion volume, $\text{kmol}/\text{m}^3 \cdot \text{s}$
 RH = parent hydrocarbon
 t = time, s
 T = absolute temperature, K
 V_L = liquid volume, m^3
 V_{GL} = dispersion volume, m^3
 x = distance in liquid from gas-liquid interface, measured along normal to interface, m
 X = cyclohexane conversion
 X_o = hypothetical initial conversion of cyclohexane at zero time
 y_i = oxygen mole fraction in inlet gases
 y_1 = oxygen mole fraction in inlet gases at $t > 0$
 y_2 = oxygen mole fraction in leaving gases at any time
 y_o = oxygen mole fraction in leaving gases initial steady state

Greek letters

α = ratio of inlet molar flow rate to outlet molar flow rate
 β = solubility of oxygen in cyclohexane, kmol/m^3
 τ_G = mean residence time of gas in contactor, s

Subscripts

I = intermediate
 o = oxygen
 P = product
 s = steady state value
 x = value at a distance x from gas-liquid interface
 z = zero-order reaction
 1 = first-order kinetics in oxygen
 0 = initial value

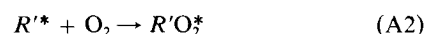
Appendix A

In the following reaction scheme for the oxidation of cyclohexane, comprising steps of initiation, propagation, and termination of free radicals, RH represents the parent hydrocarbon, PH the reaction products, R^* the primary radicals that form from either cyclohexane or the reaction products, and $R'O_2^*$ the peroxy radicals that form from R^* .

The initiation of radicals is from cyclohexane at the start of the reaction, but as the reaction products begin to build up, degenerate branching of the chains becomes important and the products increasingly become the main source of radicals (such a phenomenon is common in most hydrocarbon oxidations). After the induction period, therefore, we can write the rate of initiation as a function of the concentration of the products PH . If c_P denotes the concentration of products, then the rate of initiation, r_{ini} , is given by

$$r_{ini} = f_i(c_P) \quad (A1)$$

In the propagation step, the radicals that form in the initiation step react rapidly with oxygen to form the peroxy radicals $R'O_2^*$, which then react with cyclohexane as well as the reaction products PH . Since most reactions in the conversion of intermediate products go through the hydroperoxide stage, the products PH may be assumed to react with the radicals $R'O_2^*$ in a manner similar to cyclohexane.



Let the rate constants for reactions A2, A3, and A4 be respectively k_p , k_{p1} , and k_{p2} . Reaction A2 has a much higher rate constant than reaction A3 or A4, and hence the overall reaction is normally zero order in oxygen. In turn, k_{p1} and k_{p2} can be expected to have different values, since the products of cyclohexane oxidation, such as cyclohexanol and cyclohexanone, are more reactive than cyclohexane.

Provided the chains are of sufficient length, cyclohexane and oxygen are mainly consumed in the propagation step. We can therefore write the rate of conversion of cyclohexane from Eq. A3:

$$r_c = -\frac{dc_R}{dt} = \frac{dc_P}{dt} = k_{p1} c_R [R'O_2^*] \quad (A5)$$

where c_R , the concentration of cyclohexane, changes so little over the narrow range of conversions of interest that it may be taken as approximately constant in the term on the righthand

side. These equations are true for a batch system in which there is no net removal or addition of the cyclohexane or products, from or to the reactor. One mole of products has been assumed to form from one mole of cyclohexane. The rate of oxygen conversion follows from Eq. A2:

$$r_o = k_p c_L [R'^*] \quad (\text{A6})$$

Termination of radicals takes place by various mechanisms. In general, we consider the rate of termination r_{ter} to be a function of the total radical concentration, $[R'^* + R'O_2^*]$:

$$r_{ter} = f_t \{ [R'^*] + [R'O_2^*] \} \quad (\text{A7})$$

In order to determine the radical concentrations that enable a calculation of the rates of conversion of cyclohexane and oxygen by Eq. A5 and A6, we make the following quasi-stationary state assumption. As the radicals increase in concentration, their rate of termination also increases and we can expect the radical concentration to reach a steady state in which the rate of initiation and termination are equal. This steady state concentration of radicals is given from Eqs. A1 and A7 as a function of the total product concentration:

$$[R'^* + R'O_2^*]_s = \frac{f_i}{f_t} C_p \quad (\text{A8})$$

When the oxygen concentration is high, the R'^* radicals are effectively scavenged, and the free radicals exist predominantly in their peroxy form. We also know from the experimental results that the cyclohexane conversion rate under these circumstances is proportional to the concentration of products, c_p . Since Eq. A5 shows this rate to be proportional to the concentration of $R'O_2^*$ radicals, we can write, making the quasi-steady state assumption:

$$[R'^* + R'O_2^*]_s = [R'O_2^*]_s = K c_p \quad (\text{A9})$$

In view of this result, we assume the functional relationship expressed in Eq. A8 to be linear

$$[R' + R'O_2^*]_s = K c_p \quad (\text{A10})$$

Equating the rate of formation of radicals R'^* by reactions A3 and A4 to the rate of their consumption by reaction A2 (when the chains are long, for each occurrence of the initiation and termination reactions, there will be many occurrences of the propagation reactions, hence the rates at which radicals form and disappear can be neglected in the following equation) to evaluate the steady state concentration of these radicals:

$$k_p [R'^*]_s c_L = k_{p1} c_R [R'O_2^*]_s + k_{p2} c_P [R'O_2^*]_s \quad (\text{A11})$$

which gives

$$\frac{[R'^*]_s}{[R'O_2^*]_s} = \frac{k_{p1} c_R + k_{p2} c_P}{k_p c_L} \quad (\text{A12})$$

Using the steady state concentrations of radicals given by Eqs. A10 and A12 in Eqs. A5 and A6, we can write the rates of

cyclohexane and oxygen conversion as

$$r_c = \frac{k_{01} k_3 c_P c_L}{(k_{01} + k_{02} c_P + k_3 c_L)} \quad (\text{A13})$$

$$r_o = \frac{k_3 c_L c_P (k_{01} + k_{02} c_P)}{(k_{01} + k_{02} c_P + k_3 c_L)} \quad (\text{A14})$$

where the modified rate constants are now given by,

$$k_{01} = K k_{p1} c_R; \quad k_{02} = K k_{p2}; \quad k_3 = K k_p \quad (\text{A15})$$

Since the concentration of cyclohexane varies but little in the narrow range of conversions being studied, it has been included in the rate constant group k_{01} . The reason this constant should be the same as that obtained from a semilogarithmic plot of conversion-time data in the region of high oxygen concentrations will become apparent when the limiting case of the kinetics under conditions of high oxygen concentrations is considered. Equation A14 shows the rate of oxygen consumption to be equal to the sum of two terms, the first being due to consumption by cyclohexane and the second to consumption by the reaction products themselves.

Appendix B

Both the gas and liquid phases are assumed to be well mixed. The equations expressing the variation of the dissolved and gas phase oxygen, and the concentrations of the total products and intermediates are:

$$\frac{d(N_G y_2)}{dt} = G_1 y_1 - G_2 y_2 - k_L a V_L (c_o^* - c_L) \quad (\text{B1})$$

$$\frac{dc_L}{dt} = k_L a (c_o^* - c_L) - r_o \quad (\text{B2})$$

$$-\frac{dc_R}{dt} = \frac{dc_P}{dt} = r_c \quad (\text{B3})$$

$$\frac{dc_I}{dt} = r_i \quad (\text{B4})$$

with r_c , r_o , and r_i being given by Eqs. A13, A14, and 10, respectively. The initial conditions, at a specified time after the end of the induction period (for the kinetic model is only applicable after a certain concentration of products has been built up) are:

$$\text{at } t = 0, \quad y_2 = y_0, \quad c_L = c_{L0}, \quad c_{P0} \quad \text{and} \quad c_I = c_{I0} \quad (\text{B5})$$

These equations and initial conditions can be cast in the dimensionless form making use of the following dimensionless groups as variables:

$$\begin{aligned} A &= k_L a \tau_G; \quad B = \beta V_L / N_G; \quad C = \frac{k_{01}}{k_L a}; \\ D &= \frac{k_{02} c_i^*}{k_L a}; \quad F = \frac{k_3 c_i^*}{k_L a}; \quad \bar{t} = k_L a t; \\ \bar{y} &= \frac{Y_2}{(y_1/\alpha)}; \quad \bar{c}_L = \frac{c_L}{c_i^*}; \quad \bar{c}_P = \frac{c_P}{c_i^*}; \quad \bar{c}_I = \frac{c_I}{c_i^*} \end{aligned} \quad (\text{B6})$$

where y_i is the oxygen level at the inlet and c_i^* is the saturation concentration of dissolved oxygen at the outlet partial pressure if all the oxygen entering the contactor leaves without any being absorbed; that is, $c_i^* = \beta y_i / \alpha$.

The equations can be written, after introducing the rate expressions, as

$$\frac{d\bar{y}}{d\bar{t}} = \frac{1 - \bar{y}}{A} - B(\bar{y} - c_L) \quad (\text{B7})$$

$$\frac{d\bar{c}_L}{d\bar{t}} = \bar{y} - \bar{c}_L - F\bar{c}_L\bar{c}_p \frac{\bar{C} + D\bar{c}_p}{(\bar{C} + D\bar{c}_p + F\bar{c}_L)} \quad (\text{B8})$$

$$\frac{d\bar{c}_p}{d\bar{t}} = F\bar{c}_L\bar{c}_p \frac{\bar{C}}{(\bar{C} + D\bar{c}_p + F\bar{c}_L)} \quad (\text{B9})$$

$$\frac{d\bar{c}_i}{d\bar{t}} = F\bar{c}_L\bar{c}_p \frac{\bar{C} - D\bar{c}_i}{(\bar{C} + D\bar{c}_p + F\bar{c}_L)} \quad (\text{B10})$$

The initial conditions, in dimensionless terms, are:

$$\bar{t} = 0, \quad \bar{y} = \frac{y_o}{(y_i/\alpha)} = \bar{y}_0, \quad \bar{c}_L = \frac{c_{L0}}{c_o^*} = \bar{c}_{L0},$$

$$\bar{c}_p = \frac{c_{p0}}{c_o^*} = \bar{c}_{p0}, \quad \bar{c}_i = \frac{c_{i0}}{c_o^*} = \bar{c}_{i0} \quad (\text{B11})$$

Analytical solutions could not be obtained to the set of nonlinear differential Eqs. B7–B10 in the general case. However, when the kinetics are zero order in oxygen, the equations become linear and can be solved. Further simplicity of solutions results when one notes that a pseudosteady-state assumption can be made in the gas phase, since the gas phase transients are much faster (in view of the small gas volume and the small residence time of the gas) than the variation of the absorption rate with time. Setting the time derivative in Eq. B7 to zero and solving the resulting equations, we have the following solutions for the case of zero-order kinetics in oxygen:

$$\bar{c}_p = \bar{c}_{p0} \exp(\bar{C}\bar{t}) \quad (\text{B12})$$

$$\bar{c}_i = (\bar{C}/\bar{D}) + (\bar{c}_{i0} - \bar{C}/\bar{D}) \exp\{(\bar{D}/\bar{C})\bar{c}_{p0}[1 - \exp(\bar{C}\bar{t})]\} \quad (\text{B13})$$

$$\bar{c}_L = 1 + (\bar{c}_{L0} - 1) \exp[-\bar{t}/(1 + AB)]$$

$$- \frac{\bar{C}\bar{c}_{p0}}{[1 + \bar{C}(1 + AB)]} \{\exp(\bar{C}\bar{t}) - \exp[-\bar{t}/(1 + AB)]\}$$

$$- \frac{\bar{D}\bar{c}_{p0}^2(1 + AB)}{[1 + 2\bar{C}(1 + AB)]} \cdot \{\exp(2\bar{C}\bar{t}) - \exp[-\bar{t}/(1 + AB)]\} \quad (\text{B14})$$

$$\bar{y} = (1 + AB\bar{c}_L)/(1 + AB) \quad (\text{B15})$$

The absorption rate can be calculated from the dimensionless exit oxygen mole fraction as

$$R_A = (G_i y_i / V_{GL})(1 - y) \quad (\text{B16})$$

The assumption of pseudosteady state for the gas phase is easily checked by comparing the above solutions with the solutions for the complete set of equations. For the values of the parameters that arise in the present experiments, the solutions matched very well.

The liquid phase transients were also found to be negligible compared with the absorption rates from the experimental data. Such a pseudosteady-state assumption on the liquid phase yields, for the dissolved oxygen concentration,

$$\bar{c}_L = 1 - \bar{C}\bar{c}_{p0}(1 + AB) \exp(\bar{C}\bar{t}) - \bar{D}\bar{c}_{p0}^2(1 + AB) \exp(2\bar{C}\bar{t}) \quad (\text{B17})$$

Because Eq. B17 is always valid, at least in an approximate sense, the initial conditions at $t = 0$ are not all independent of one another. Once an initial product composition is specified, the reaction rate and hence the absorption rate are determined, and the system determines its own dissolved oxygen concentration, depending on the volumetric mass transfer coefficient, so that oxygen can be transferred at the required rate into the liquid.

Literature Cited

- Astarita, G., *Mass Transfer with Chemical Reaction*, Elsevier, Amsterdam (1967).
- Berezin, I. V., E. T. Denisov, and N. M. Emanuel, *The Oxidation of Cyclohexane*, K. A. Allen, trans., Pergamon, Oxford (1966).
- Botton, R., D. Cossier, F. Vergnes, and J. C. Charpentier, "Conception Extrapolation et Ameliorations Potentielles de Certains Reacteurs de l'Industrie Chimique. Une Analyse Generale et Quelques Exemples Vecus," *Entropie*, No. 109, 4 (1983).
- Emanuel, N. M., E. T. Denisov, and Z. K. Maizus, *Liquid-Phase Oxidation of Hydrocarbons*, Plenum, New York (1967).
- Emanuel, N. M., "The Kinetic Features of the Chain Mechanism of Liquid-Phase Oxidation Process," *Problems in Chemical Kinetics*, N.M. Emanuel, ed., Artavaz Brehnazarov, trans., Mir Pub., Moscow (1981).
- Katnik, R. J., and G. V. Johnston, "Gas Chromatographic Analysis of Cyclohexane Oxidation Products," *J. Chromat. Sci.*, **8**, 543 (1970).
- Suresh, A. K. (Suresh A. Krishnamurthy), "Mass Transfer and Chemical Reaction in Cyclohexane Oxidation," Ph.D. Thesis, Dept. Chem. Eng., Monash Univ., Clayton, Australia (1986).
- Suresh, A. K., T. Sridhar, and O. E. Potter, "Mass Transfer and Solubility in Autocatalytic Oxidation of Cyclohexane," *AIChE J.*, **33**(12) (Dec., 1987).
- Takamitsu, N., and T. Hamamoto, "Autoxidation of Cyclohexane in the Presence of Fatty Acids and Decomposition of Cyclohexyl Hydroperoxide," *Nippon Kagaku Kaishi*, **9**, 1587 (1972).
- van de Vusse, J. G., "Mass Transfer with Chemical Reaction," *Chem. Eng. Sci.*, **16**, 21 (1961).

Manuscript received July 22, 1986, and revision received July 13, 1987.